ACS APPLIED POLYMER MATERIALS

pubs.acs.org/acsapm Article

Flexible and Highly Sensitive Sandwich-Structured PDMS with Silver Nanowires and Laser-Induced Graphene for Rapid Residue Detection

Lin Cheng, Jinchen Qian, Diqing Ruan, Guanzheng Chen, Jiayao Yang, Huaping Wu, and Aiping Liu*

Cite This: ACS Appl. Polym. Mater. 2023, 5, 2336−2344 Read Online

ACCESS | Metrics & More | Article Recommendations | Supporting Information

ABSTRACT: Flexible surface-enhanced Raman scattering (SERS) substrates offer advantages over traditional rigid substrates for efficient extraction of target molecules from complex surfaces, which is critical for technical applications ranging from pesticide residue analysis to environmental pollutant monitoring and forensic science detection. Herein, flexible sandwich-structured silver nanowires with laser-induced graphene and polydimethylsiloxane (PDMS) (Ag NWs@LIG@PDMS) with high SERS activity, flexibility, and stability were prepared by a simple method. Its detection limit is as high as 10^{-14} M, which is significantly higher than that of silver nanowires embedded in PDMS (Ag NWs/PDMS) and silver nanowire adhesive PDMS (Ag NWs@PDMS) with bilayer structure, due to the efficacy of interlayer laser-induced graphene (LIG). Moreover, compared with similar structures, the sophisticated structural design of silver nanowires with laser-induced graphene embedded in PDMS (Ag NWs/LIG@PDMS) enables higher SERS activity. Apart from this, the Ag NWs@LIG@PDMS film maintains excellent SERS performance even under 10% tensile deformation and extreme operating temperature (−80 to 80 °C). In view of the above-mentioned advantages, SERS substrates have been successfully used for fast, efficient, low-cost, and nondestructive extraction and detection of peel surface and fingerprint residues in real scenes, providing avenues for molecular trace extraction and detection in food safety and forensics science.

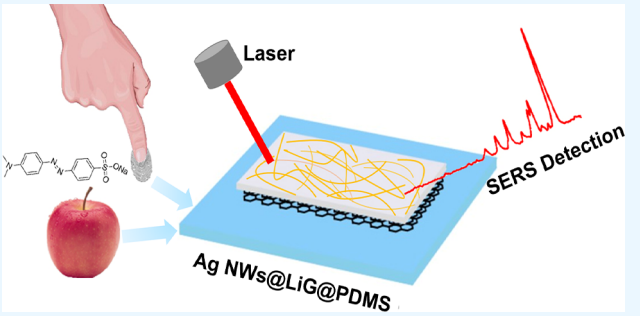

KEYWORDS: *laser-induced graphene, Ag NWs, sandwich structure, surface-enhanced Raman scattering, residue detection*

Downloaded via ZHEJIANG SCI-TECH UNIV on May 2, 2024 at 12:51:51 (UTC).
See https://pubs.acs.org/sharingguidelines for options on how to legitimately share published articles.

1. INTRODUCTION

Surface-enhanced Raman scattering (SERS) is an advanced spectroscopic detection technology for tracing molecules, which can effectively improve signal intensity. Therefore, it has a wide range of applications in food safety, biomedical research, environmental monitoring, medical safety, intelligent sensing, and other fields.[1−5] Its unique advantages such as nondestruction, ultrasensitive detection limit, fingerprint information, and easy operation show irreplaceable value.[6−9] In fact, the detection performance of SERS technology in these applications usually depends on the choice of SERS substrate. Thus, the selection of material, the design of morphology, and structure of SERS substrate are crucial for the advancement and application of this technology.

According to the SERS enhancement mechanism, silver is considered as the preferred SERS material.[10] In recent research of related fields, other researchers have prepared a series of Ag-based SERS substrates, such as 3D silver nanoparticles,[11] Au−Ag core−shell nanorods,[12] flower-like Ag@molecularly imprinted polymers,[13] PS/Cu_2S/Ag sandwich substrates,[14] flexible Ag−nanocubes@PE film,[15] flexible Ag nanotree@Cu mesh SERS substrate,[16] and so on. But in general, according to the hardness of the substrate, Ag-based SERS substrates are mainly divided into two categories. The first category is generally made of smooth and rigid glass sheets or silicon wafers to support silver materials, but such strong and inflexible substrates are often limited to laboratory tests and are not convenient for practical applications in real complex surfaces. On the contrary, the second category of Ag-based SERS substrates, i.e., the flexible SERS, can be attached to different target surfaces and can be easily peeled off from the surface of the object via a simple "paste and peel off" approach, hardly causing damage to the surface of the object. The emerging flexible substrate materials such as paper, fiber, adhesive tape, and polymer materials have been introduced into the development of Ag-based SERS substrates with an incredible potential.[17−20] For instance, Lin et al.[17] developed a paper-based dual-functional SERS platform for effective and

Received: November 20, 2022
Accepted: March 6, 2023
Published: March 13, 2023

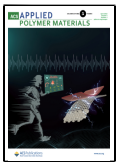

ACS Publications © 2023 American Chemical Society

https://doi.org/10.1021/acsapm.2c02011
ACS Appl. Polym. Mater. 2023, 5, 2336−2344

reliable measurements of thiram on complex surfaces. Lu et al.[18] reported a 3D Ag nanodendrites/carbon fiber cloth substrate, which showed the lowest concentration of crystal violet (CV) for 10^{-10} M. Gong et al.[19] reported a simple and rapid SERS detection method by applying Ag NPs to the surface of the tape after analyte collection. Luo et al.[20] constructed a flexible silver nanowires embedded in PDMS (Ag NWs@PDMS) with excellent SERS activity, durability, and recyclability. Obviously, these flexible Ag-based SERS substrates allow direct collection of residues on irregular and rough surfaces in a noninvasive manner, which is more suitable for practical applications. However, the physical enhancement of Ag SERS substrates alone may not meet the higher detection requirements.

Because graphene-enhanced Raman scattering (GERS) was proposed by Ling et al.,[21] the further exploration of graphene-based surface Raman enhancement has opened up a new research direction for practical SERS applications.[22−24] Liang et al. demonstrated that graphene had a fluorescence quenching effect and could be used for electromagnetic and chemical dual enhancement of metal−nanostructure interactions.[25] However, current synthesis methods of graphene require either high-temperature processing or multistep chemical synthesis routes, lessening their widespread commercial potential. Laser-induced graphene (LIG), prepared by direct laser writing on some polymer materials, has the advantages of simple preparation, easy graphic design, low cost, and excellent physicochemical properties.[26] Its potential as a potential material for SERS substrates has not yet been fully unlocked.

In this contribution, we propose an economical, simple, and rapid method to fabricate sandwich structured silver nanowires with laser-induced graphene and polydimethylsiloxane (PDMS) (Ag NWs@LIG@PDMS) with LIG as the intermediate layer, Ag NWs as the functional layer, and PDMS as the flexible substrate layer. The SERS substrate exhibits ultrasensitive detection of Rhodamine 6G (R6G) with a detection limit of 10^{-14} M. Meanwhile, the SERS substrate also exhibits good uniformity, anti-interference, tensile strength, long-term reliability, and the capability of operating in ultimate temperatures. To further demonstrate the advantages of Ag NWs@LIG@PDMS, the SERS performances of three similar structures of silver nanowires with laser-induced graphene embedded in PDMS (Ag NWs/LIG@PDMS), silver nanowires embedded in PDMS Ag NWs/PDMS, and silver nanowire adhesive PDMS (Ag NWs@PDMS) were also compared. The results demonstrated that the LIG interlayer could promote the deposition and stabilization of Ag NWs,[26,27] and the sophisticated structural design of Ag NWs@LIG@PDMS enabled the substrate to have the combined effect of Ag electromagnetic enhancement and LIG chemical enhancement, showing highly sensitive SERS activity. Notably, the flexible and highly sensitive SERS substrate enabled detection of organic residues on noninvasive peel surfaces by in situ surface wiping. Furthermore, satisfactory SERS signal feedback was also obtained by using this SERS substrate to detect residues in fingerprints.

2. EXPERIMENTAL SECTION

2.1. Preparation of Ag NWs@LIG@PDMS Flexible SERS Substrate. First, LIG with fluffy structure was fabricated on a PI film using CO_2 laser at the scanning speed of 18 mm/s and a frequency of 100 kHz. Second, an appropriate amount of PDMS and curing agent were mixed on the surface of LIG and then were cured at 130 °C for 1 h. Subsequently, the PI film was gently peeled off to obtain a LIG@PDMS film. Finally, Ag NWs (5 mg/mL in isopropanol) were evenly spin-coated on the surface of the LIG@PDMS flexible substrate (20 mm × 10 mm) and were then air-dried at room temperature to obtain a sandwich-structured Ag NWs@LIG@PDMS film.

2.2. Preparation of Ag NWs/LIG@PDMS Flexible SERS Substrate. Different from Ag NWs@LIG@PDMS, the preparation of Ag NWs/LIG@PDMS films was directly spin-coated on the LIG layer with 100 μL of Ag NWs, followed by a mixture of PDMS. The Ag NWs surface was covered uniformly with the curing agent. After PDMS curing, the PI film was peeled off to obtain the Ag NWs/LIG@PDMS flexible SERS substrate.

2.3. Preparation of Embedded Ag NWs/PDMS Film. 2 mL of Ag NWs suspension was dropped and uniformly dispersed on a clean glass slide (75 mm × 25 mm) and was then air-dried. Next, an appropriate amount of the mixture of PDMS and curing agent was uniformly covered on the surface of Ag NWs and was cured at 130 °C for 1 h. Finally, the embedded Ag NWs/PDMS was peeled off from the glass slide.

2.4. Preparation of Adhesive Ag NWs@PDMS Film. First, the PDMS mixed solution was spread on a glass slide and cured, and then the Ag NWs suspension was drop-coated on the PDMS film. After being dried, the Ag NWs@PDMS films were peeled off from the glass slides.

2.5. SERS Detection. For SERS limit detection, Ag NWs@LIG@PDMS SERS substrate was immersed in R6G aqueous solutions at different concentrations for SERS measurements. Furthermore, similar dyes (CV and MB) at the same concentration (10 μM) were added to a 10 μM solution of R6G, after which the Ag NWs@LIG@PDMS films were immersed in a solution spiked with interfering substances and were later used for SERS measurements. For uniformity testing, five batches of Ag NWs@LIG@PDMS films were immersed in 1 μM R6G solution, and different sites were characterized on different batches of films. Furthermore, 20 sites were randomly selected for SERS measurements on one of the films. For the tensile property test of the film material, the film adsorbed with 1 μM R6G was stretched to about 10% of its length for a certain number of times to conduct the SERS measurement. To investigate the effect of extreme operating temperatures on SERS substrates, the Ag NWs@LIG@PDMS films immersed in 1 μM R6G were treated under harsh temperature (−80 °C low temperature and 80 °C high temperature) for 12 h before the measurement. For oxidation resistance and stability tests, SERS measurements were performed in a natural environment at 30-day intervals using Ag NWs@LIG@PDMS films adsorbed with 1 μM R6G. For the fruit peel surface detection experiment, 20 μL of R6G solution at different concentrations was dropped on the fruit peel surface (0.8 × 2 cm^2). After the solution evaporated naturally, the prepared flexible Ag NWs@LIG@PDMS were soaked in ethanol and wiped on the fruit surface to collect contaminants from the fruit surface. The wiped SERS substrates were subjected to SERS testing at three random points. For residue detection in fingerprints, SERS detection was performed by dropping R6G droplets with 20 μL on the finger, and after the finger dried naturally, it is pressed on the prepared Ag NWs@LIG@PDMS film.

2.6. Characterization. The micromorphological features were characterized by a field emission scanning electron microscope (FE-SEM, Hitachi S4800). The crystalline structure was investigated by an X-ray diffractometer (Bruker AXS D8) using the Cu Kα radiation (λ = 0.15418 nm) with the 2θ scan from 10° to 80° at a step of 0.02°. Elemental analysis was performed by X-ray photoelectron spectroscopy (XPS) using a Thermo Fisher Scientific ESCALAB Xi+ instrument with an Al Kα radiation source. Raman analysis was conducted using a Renishaw inVia-Reflex Raman microscope at room temperature under 532 nm laser, 0.1 W laser power, and 50× (NA = 0.90) objective.

https://doi.org/10.1021/acsapm.2c02011
ACS Appl. Polym. Mater. 2023, 5, 2336−2344

Scheme 1. Schematic Diagram of the Fabrication of Ag NWs@LIG@PDMS SERS Substrate

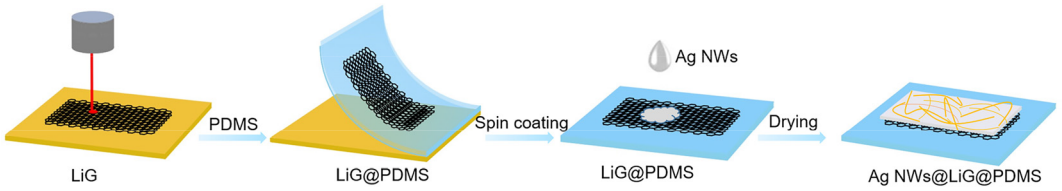

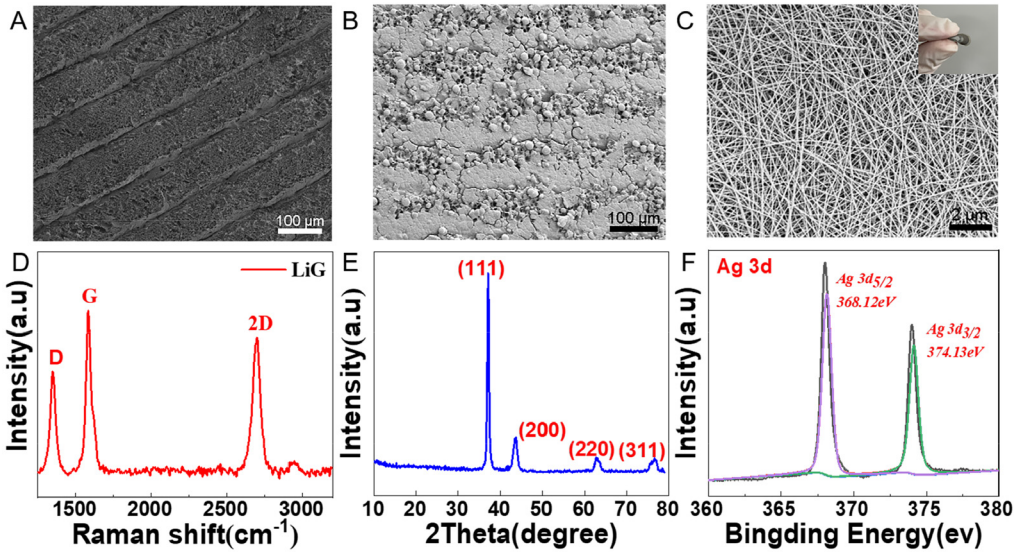

Figure 1. (A) SEM images of LIG, (B) LIG@PDMS, and (C) Ag NWs@LIG@PDMS films. (D) SERS of LIG. (E) XRD and (F) XPS of Ag NWs@LIG@PDMS.

3. RESULTS AND DISCUSSION

3.1. Characterization of Ag NWs@LIG@PDMS. The Ag NWs@LIG@PDMS sandwich structure film was prepared as shown in Scheme 1. First, LIG was prepared on PI film by a CO_2 laser. Then, by peeling off the PI film, the LIG@PDMS film was obtained. Finally, Ag NW was spin-coated on the surface of LIG@PDMS flexible substrate to obtain the Ag NW@LIG@PDMS film with sandwich structure. As is shown in Figure 1A, the surface of the LIG film on the PI film was regular and uniform, the channels of laser printing were neatly distributed, and the LIG presented a fluffy and porous structure. The Raman spectrum of LIG (Figure 1D) suggests three prominent peaks of graphene: D peak (about 1360 cm^{-1}), G peak (about 1580 cm^{-1}), and 2D peak (2665 cm^{-1}). Among them, the D peak resulted from defects or bent sp^2-carbon bonds (bent graphene layers), and the low D/G intensity ratio indicated a high degree of graphene crystallinity of LIG.[27−29] Then, LIG was transferred to the flexible PDMS, which is displayed in Figure 1B. The porous structure of the LIG was clearly visible, and the transferred film still maintained good uniformity. As illustrated in Figure 1C, Ag NWs were interconnected to form a multilayer network and were uniformly attached to the surface of LIG@PDMS after the transfer step. The inset is an optical image showing the flexibility and softness of the sample. Its sandwich structure is shown in the cross-sectional SEM in Figure S2A. The top layer was Ag NWs, the middle porous layer was LIG, and the bottom layer was the support layer PDMS. The inset clearly shows the dense and neat arrangement of Ag NWs layer, and the LIG layer was well supported. The XRD pattern of Ag NWs (Figure 1E) showed characteristic diffraction peaks at 2θ of 38.2°, 44.5°, 64.5°, and 77.5°, corresponding to (111), (200), (220), and (311) silver face-centered cubic crystal phase (JCPDS 04-0783).[30] The XPS Ag 3d spectrum (Figure 1F) confirmed the successful deposition of Ag NWs, with peaks at 368.12 and 374.13 eV corresponding to the binding energies of Ag $3d_{5/2}$ and Ag $3d_{3/2}$ of Ag(0).[31]

Considering that the Ag NWs layer will affect the SERS signal, 50, 100, and 150 μL of Ag NWs (5 mg/mL) were used for the comparison experiments. The corresponding SEM (Figure S1) shows that when the amount of Ag NWs was insufficient (50 μL), it was not enough to cover the LIG layer (Figure S1A). In contrast, when it increased to 100 μL, the Ag NWs completely covered the LIG layer (Figure S1B), and the surface of the layer showed uniformity and integrity in a large area. Correspondingly, the SERS signal intensity increased with the increase of Ag NWs density (Figure 2A). However, the 150 μL Ag NWs resulted in severe cracks on the surface (Figure S1C) which would lead to a decrease in the reproducibility and stability of the SERS signal. Accordingly, 100 μL of Ag NWs (5 mg/mL) at 0.25 mg/cm^2 was selected for the subsequent experiments.

Furthermore, to confirm the advantages of the sandwich structure, we compared the SERS signal intensity of the sandwich structure with three other structures (the adhesive Ag NWs/LIG@PDM with similar sandwich structure, the embedded Ag NWs/PDMS, and the unwrapped Ag NWs@PDM) (Figure 2B). Under the same conditions (1 μM R6G solution), the SERS signal intensity of Ag NWs@LIG@PDMS film was significantly higher than that of the other three similar structures. And the SERS detection limit was also the highest, which could detect 10^{-14} M R6G solution (Figure 2C)

https://doi.org/10.1021/acsapm.2c02011
ACS Appl. Polym. Mater. 2023, 5, 2336−2344

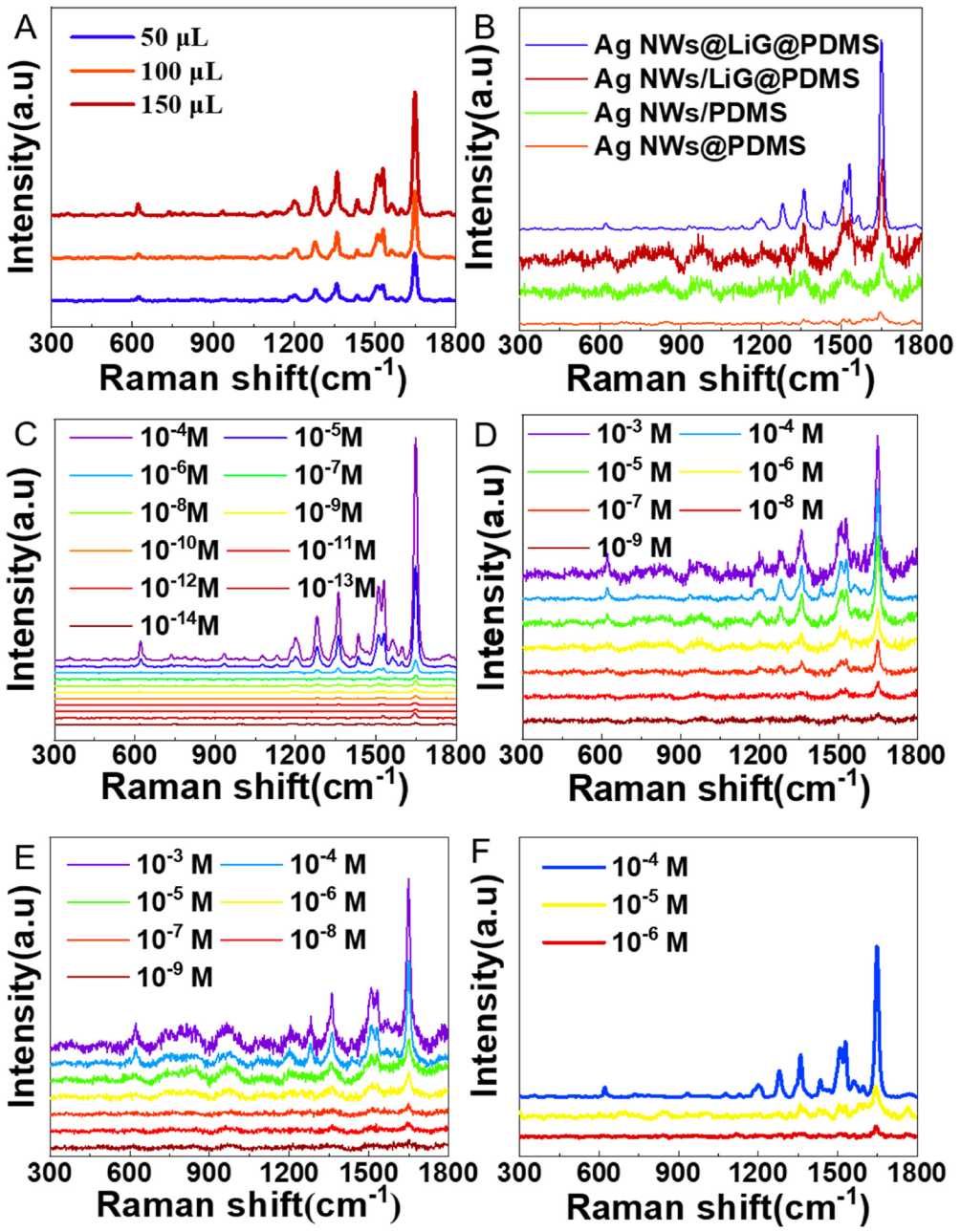

Figure 2. (A) SERS spectra of Ag NWs@LIG@PDMS with different Ag NWs density. (B) SERS spectra of 1 μM R6G adsorbed on Ag NWs@LIG@PDMS, Ag NWs/LIG@PDMS, Ag NWs/PDMS, and Ag NWs@PDMS. SERS spectra of R6G with different concentrations on Ag NWs@LIG@PDMS (C), Ag NWs/LIG@PDMS (D), Ag NWs/LIG (E), and Ag NWs@LIG (F).

Table 1. Recent Progress of the Ag NWs-Based SERS-Active Substrates for Detecting the Trace Amount of Analytes

material	analyte	LOD (M)	EF	flexibility[a]	ref
Ag NWs/PS fibers	4-ATP	10^{-7}	10^{-5}	√	34
Ag/Au NWs/PDMS	2- naphthalenethiol	10^{-10}	6.74×10^{6}	√	35
ZIF-67@Ag NWs	DBP	3×10^{-13}	8.9×10^{7}	×	36
Ag NWs@PDMS	MG	10^{-8}	4.77×10^{5}	√	20
Au NP/Ag NWs/PU	MG	10^{-10}	10^{3}	√	37
Au NRs/Ag NWs	R6G	10^{-12}		×	38
Ag NW-Ag NP-MoS_2	R6G	10^{-11}	2.6×10^{6}	×	39
Ag NWNFs/PDMS	R6G	10^{-7}		√	40
Ag NWs/LIG@PDMS	R6G	10^{-9}	7.8×10^{6}	√	this work
Ag NWs@LIG@PDMS	R6G	10^{-14}	9.96×10^{6}	√	this work

[a]√ indicates that the material is flexible. × indicates that the material is not flexible

https://doi.org/10.1021/acsapm.2c02011
ACS Appl. Polym. Mater. 2023, 5, 2336−2344

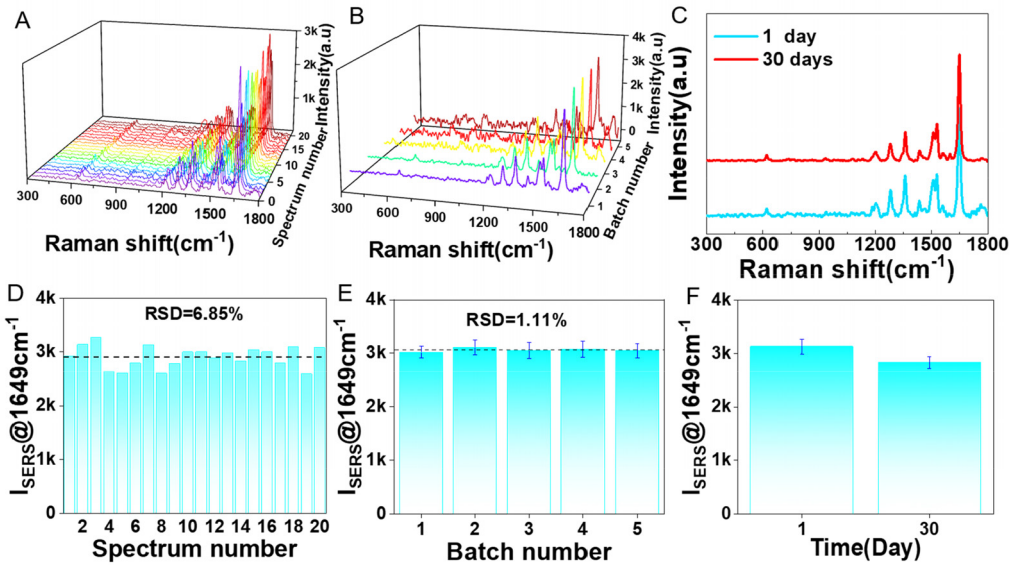

Figure 3. SERS spectra of R6G measured on Ag NWs@LIG@PDMS for (A) point-to-point uniformity on 20 random positions. (B) Batch-to-batch uniformity with five batches. (C) SERS stability at 30-day intervals. (D–F) Corresponding peak intensities at 1649 cm^{-1}.

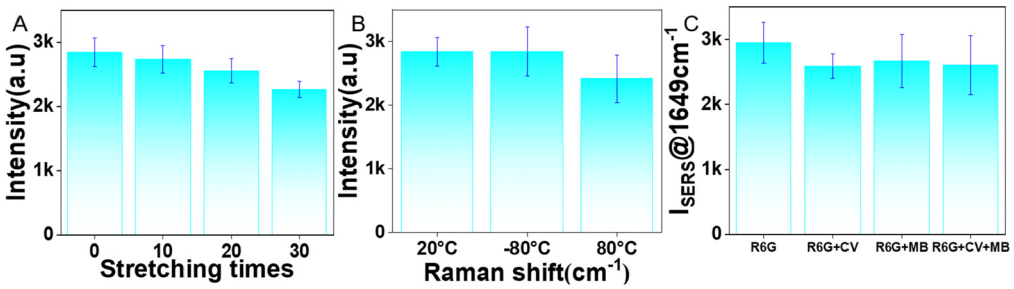

Figure 4. (A) Peak intensity of the SERS spectrum at 1649 cm^{-1} at different stretching times, (B) at different working temperatures, and (C) with CV and MB interference.

compared with 10^{-9} M for Ag NWs/LIG@PDMS film with a similar sandwich structure (Figure 2D); the embedded Ag NWs/PDMS film had a higher detection limit (Figure 2E) than the unwrapped Ag NWs@PDMS (10^{-6} M) (Figure 2F). The sandwich structure was obviously better than the two-layer structure for the chemical enhancement produced by the LIG layer enhanced the SERS signal (Figure S4), which further proves that the introduction of LIG not only had the effect of enhancing SERS but also could inhibit the side reactions and fluorescence quenching.[32,33] The cross-sectional views of the four structures are shown in Figure S2, where the positions marked in red are the embedded Ag NWs layers. Figures S2B and S3A show that the upper layer of the Ag NWs/LIG@PDM was LIG, and the middle was wrapped by the Ag NWs, which limited the enhancement of Ag SERS signal, thus resulting in weaker SERS signal than sandwich structure Ag NWs@LIG@PDMS. The embedded Ag NWs/PDMS film was found to have better SERS signal than the unwrapped Ag NWs@PDMS (Figure S3B) due to the hydrophobic interaction of the flexible PDMS, which could concentrate the analytes and thus enhance the SERS signal.[20] Furthermore, the unwrapped Ag NWs@PDMS only relied on the adhesion of the PDMS layer to maintain the Ag layer, and the surface layer was easily damaged and wrinkled (Figure S2C). Compared with the Ag NW-based SERS substrates reported in the current literature (Table 1), the sandwich-structured Ag NWs@LIG@PDMS had a detection limit far superior to those reports in most literature.[34−40,20] Figure S5 shows the SERS spectrum of 10^{-6} M R6G adsorbed on Ag NWs@LIG@PDMS and the Raman spectrum of 10^{-2} M R6G aqueous solution. So the commonly used enhancement factor (EF) value was obtained as 9.96×10^6 through the detailed calculation of Supporting Information S1.[41] Compared with other literature, the prepared substrate has relatively high enhancement factors.[34−40,20]

3.2. SERS Performance of Ag NWs@LIG@PDMS Flexible Film. Signal uniformity and stability are the main concerns for the SERS substrate. Therefore, 20 locations were randomly selected from the prepared flexible film to examine the point-to-point uniformity (Figure 3A), and a slight variation of the peak intensity at 1649 cm^{-1} was observed with a low relative standard deviation (RSD) of 6.85% (Figure 3D). Meanwhile, the batch-to-batch uniformity is shown in Figure 3B, and a low RSD value of about 1.11% was obtained experimentally (Figure 3E).

In routine use and line transportation, storage stability should also be considered, as Ag NWs may be easily oxidized during long-term storage.[42] Figure 3C and F shows that the peak intensity at 1649 cm^{-1} remained at 88.44% of the initial strength after 30 days (Figure 3. Excellent SERS stability was also confirmed by XPS analysis (Figure S6). R6G as an organic dye has photobleaching, which is responsible for the instability

https://doi.org/10.1021/acsapm.2c02011
ACS Appl. Polym. Mater. 2023, 5, 2336−2344

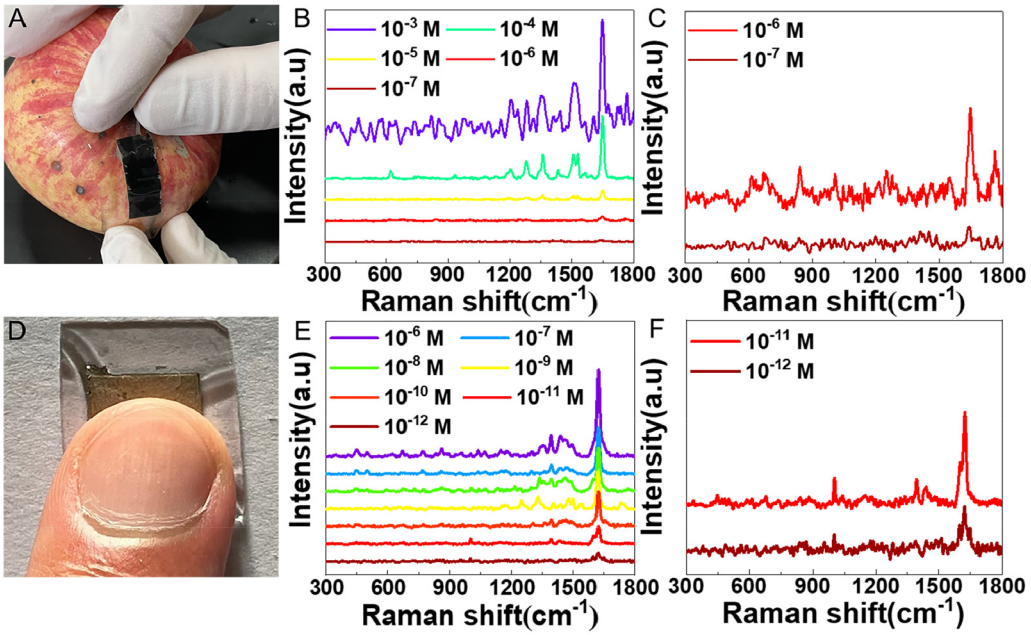

Figure 5. (A) Image of residues extracted from apple peel. (B) SERS spectra of R6G residues on the peel surface. (C) Enlarged spectral lines of R6G for 10^{-6} and 10^{-7} M from (B). (D) Image of finger pressing. (E) SERS spectra of R6G obtained by the fingerprint. (F) Enlarged spectral lines of R6G for 10^{-11} and 10^{-12} M from (E).

of SERS. Although Ag nanostructures can generate hot spots and achieve a good SERS effect, the hot spots also enhance the photobleaching effect of dye molecules.[43] Fortunately, the unique design of the sandwich-structured Ag NWs@LIG@PDMS and the fluffy LIG layer reduce the possibility of photobleaching, thereby enhancing the photostability.[44] Simultaneously, LIG may have the advantage of suppressing side reactions and fluorescence quenching.[45]

In addition to the attractive SERS sensitivity and stability, the developed Ag NWs@LIG@PDMS flexible film also exhibited stretch resistance, a wide operating temperature range, and anti-interference ability. Specifically, the Ag NWs@LIG@PDMS film was stretched and deformed more than 10% without breaking (Figure S7A); it still had a high-intensity signal after being stretched 30 times (Figure 4A) with the peak intensity remaining relatively stable at 1649 cm^{-1} (Figure S7B). Furthermore, even though the film was kept in a −80 °C refrigerator or on a heating table at 80 °C for more than 12 h, the SERS intensity was still within the ideal range (Figure 4B). Therefore, the Ag NWs@LIG@PDMS is suitable for SERS detection under complex and extreme conditions. The Ag NWs@LIG@PDMS film also has the ability to resist interference as a SERS substrate. Figure 4C show that the characteristic peaks of R6G can be effectively measured with little change in intensity by adding equal concentrations (10 μM) of CV, MB, and CV + MB to the control solution (R6G only).

3.3. SERS Substrate Application. *3.3.1. Detection of R6G on the Fruit Surface.* So far, we have demonstrated that Ag NWs@LIG@PDMS film has excellent SERS sensitivity, stability, antistretching properties, and anti-interference ability. Therefore, there is a prospect of the SERS platform being further used to analyze pesticide molecules in real scenarios. In the experiment, 20 μL R6G aqueous solutions of different concentrations (from 10^{-4} to 10^{-7} M) were added dropwise to the surface of fruits such as apples (0.5 × 0.5 cm^2), and after natural drying, the prepared Ag NWs@LIG@PDMS films were gently attached to the surface of the apple (Figure 5A). After that, the dye residue on the peel was removed immediately. The SERS intensity at 1649 cm^{-1} increased with increasing R6G concentration (Figure 5B), and even if only 10^{-7} M R6G was added to the peel surface, the SERS signal could still be identified (Figure 5C). Compared with traditional extraction methods such as microwave-assisted extraction (MAE), accelerated solvent extraction (ASE), and membrane extraction, this method is time-saving, labor-saving, simple to operate, and low-cost.[46−49] Encouragingly, the Ag NWs@LIG@PDMS is flexible and durable, so it does not damage the samples and can be reused. It achieves fast, effective, and nondestructive target extraction from the original complex object surface, which is of great significance in analytical science.

3.3.2. Portable SERS Detection in Fingerprints. The composition of human skin is complex, and residues such as drugs, additives, and pesticides derived from human social activities are also present on the skin.[50] Therefore, seeking a reliable method to detect residues in fingerprints has practical value and application prospects in forensic investigation and evidence collection. The ability of the Ag NWs@LIG@PDMS films to detect fingerprint residues under real conditions will be further evaluated. In the experiment, droplets containing 10^{-6} to 10^{-12} M R6G were taken to contaminate the fingers. After being dried, the fingers were pressed on the surface of the film (Figure 5D). Figure 5E shows that the Ag NWs@LIG@PDMS film also had excellent SERS signal characterization ability in fingerprints, even at extremely low concentrations of 10^{-12} M in R6G aqueous solution (Figure 5F). This results show that the highly sensitive Ag NWs@LIG@PDMS SERS substrate extraction process is a promising tool to extract fingerprints from crime scenes.

4. CONCLUSIONS

By combining Ag NWs, LIG, and PDMS, we designed and fabricated a flexible Ag NWs@LIG@PDMS film with high

https://doi.org/10.1021/acsapm.2c02011
ACS Appl. Polym. Mater. 2023, 5, 2336−2344

sensitivity and durability. Compared with similar structures of Ag NWs/LIG@PDMS, the sandwich-structured Ag NWs@LIG@PDMS had a higher detection limit due to its unique structural design Meanwhile, compared with the two-layered Ag NWs@PDMS and Ag NWs/PDMS, the introduction of LIG can promote not only the deposition and stabilization of Ag NWs[26,27] but also the combined effect of Ag electromagnetic enhancement and LIG chemical enhancement, showing highly sensitive SERS activity. In view of its good uniformity, flexibility, anti-interference, stability, and wide operating temperature range, the Ag NWs@LIG@PDMS film as SERS substrate was used for pesticide residue detection on the peel surface. The fast, nondestructive, and efficient extraction of residues from the original complex object surface proves great significance in the field of analysis applications. In addition, this SERS technique can also detect trace residues in fingerprints, which will be a promising tool for crime tracking in forensic science.

■ ASSOCIATED CONTENT

Supporting Information

The Supporting Information is available free of charge at https://pubs.acs.org/doi/10.1021/acsapm.2c02011.

Additional figures and data including calculation of enhancement factor EF, SEM investigations of Ag NWs@LIG@PDMS, Ag NWs/LIG@PDMS, Ag NWs/PDMS, and Ag NWs@PDMS, SERS spectrum of R6G adsorbed on Ag NWs@LIG@PDMS and R6G solution, optical images of Ag NWs@LiG@PDMS film before and after being stretched, Raman spectra of Ag NWs@LiG@PDMS films stretched for different times and treated at different temperatures (PDF)

■ AUTHOR INFORMATION

Corresponding Author

Aiping Liu − *Center for Optoelectronics Materials and Devices, Key Laboratory of Optical Field Manipulation of Zhejiang Province, School of Materials Science & Engineering, Zhejiang Sci-Tech University, Hangzhou 310018, China;* orcid.org/0000-0002-2338-062X; Email: liuaiping1979@gmail.com

Authors

Lin Cheng − *Center for Optoelectronics Materials and Devices, Key Laboratory of Optical Field Manipulation of Zhejiang Province, School of Materials Science & Engineering, Zhejiang Sci-Tech University, Hangzhou 310018, China;* orcid.org/0000-0001-8680-1383

Jinchen Qian − *Center for Optoelectronics Materials and Devices, Key Laboratory of Optical Field Manipulation of Zhejiang Province, School of Materials Science & Engineering, Zhejiang Sci-Tech University, Hangzhou 310018, China*

Diqing Ruan − *Center for Optoelectronics Materials and Devices, Key Laboratory of Optical Field Manipulation of Zhejiang Province, School of Materials Science & Engineering, Zhejiang Sci-Tech University, Hangzhou 310018, China*

Guanzheng Chen − *Center for Optoelectronics Materials and Devices, Key Laboratory of Optical Field Manipulation of Zhejiang Province, School of Materials Science & Engineering, Zhejiang Sci-Tech University, Hangzhou 310018, China*

Jiayao Yang − *Center for Optoelectronics Materials and Devices, Key Laboratory of Optical Field Manipulation of Zhejiang Province, School of Materials Science & Engineering, Zhejiang Sci-Tech University, Hangzhou 310018, China*

Huaping Wu − *Key Laboratory of Special Purpose Equipment and Advanced Processing Technology, Ministry of Education and Zhejiang Province, College of Mechanical Engineering, Zhejiang University of Technology, Hangzhou 310023, China;* orcid.org/0000-0003-4505-7062

Complete contact information is available at: https://pubs.acs.org/10.1021/acsapm.2c02011

Notes

The authors declare no competing financial interest.

■ ACKNOWLEDGMENTS

This work was supported by the National Natural Science Foundation of China (No. 12272351), the Youth Top-notch Talent Project of Zhejiang Ten Thousand Plan of China (No. ZJWR0308010), the Zhejiang Provincial Natural Science Foundation of China (No. LR19E020004 and LQ20E010009), the Fundamental Research Funds of Zhejiang Sci-Tech University (2021Q050), and the Zhejiang University Student Science and Technology Innovation Activity Plan (Xinmiao Talent Plan) Project (2022R406001).

■ REFERENCES

(1) Zou, B. F.; Wang, Y. H.; Zhou, S. M.; Yang, S. K.; Wang, Y. Q. Seed/ligand-cooperative growth of dense Au nanospikes on magnetic microparticles for SERS applications. *J. Mater. Chem. C* **2022**, *10*, 3368−3374.

(2) Zeng, Y.; Koo, K. M.; Trau, M.; Shen, A. G.; Hu, J. M. Watching SERS glow for multiplex biomolecular analysis in the clinic. *Appl. Mater. Today* **2019**, *15*, 431−444.

(3) Li, X.; Wang, X.; Liu, J.; Dai, M.; Zhang, Q.; Li, Y.; Huang, J.-A. Surface-enhanced Raman spectroscopy detection of organic molecules and in situ monitoring of organic reactions by ion-induced silver nanoparticle clusters. *Phys. Chem. Chem. Phys.* **2022**, *24*, 2826−2831.

(4) Chen, Q.; Zhao, L.; Liu, H.; Ding, Q.; Jia, C.; Liao, S.; Cheng, N.; Yue, M.; Yang, S. Nanoporous silver nanorods as surface-enhanced Raman scattering substrates. *Biosens. Bioelectron* **2022**, *202*, 114004.

(5) Zhang, S.; Lin, C.; Xia, Z.; Chen, M.; Jia, Y.; Tao, B.; Li, S.; Cai, K. A facile and novel design of multifunctional electronic skin based on polydimethylsiloxane with micropillars for signal monitoring. *J. Mater. Chem. B* **2020**, *8*, 8315−8322.

(6) Muhammad, M.; Huang, Q. A review of aptamer-based SERS biosensors: Design strategies and applications. *Talanta* **2021**, *227*, 122188.

(7) Yue, X.; Su, Y.; Wang, X.; Li, L.; Ji, W.; Ozaki, Y. Reusable silicon-based SERS chip for ratiometric analysis of fluoride ion in aqueous solutions. *ACS Sens* **2019**, *4*, 2336−2342.

(8) Li, H.; Li, C.; Martin, F. L.; Zhang, D. Diagnose pathogens in drinking water via magnetic Surface-enhanced Raman scattering (SERS) assay. *Mater. Today* **2017**, *4*, 25−31.

(9) Liu, S.; Li, H.; Hassan, M. M.; Ali, S.; Chen, Q. SERS based artificial peroxidase enzyme regulated multiple signal amplified system for quantitative detection of foodborne pathogens. *Food Control* **2021**, *123*, 107733.

(10) Chen, Y.; Liu, H.; Li, X.; Tang, S.; Gu, C.; Wei, G.; Jiang, T.; Zhou, X. Development of RGO@MoS_2@Ag ternary nanocomposites

with tunable geometry structure for recyclable SERS detection. *Sens. Actuators B Chem.* **2021**, *339*, 129856.
(11) Li, Z.; Jiang, S.; Huo, Y.; Ning, T.; Liu, A. H.; Zhang, C.; He, Y.; Wang, M.; Li, C.; Man, B. silver nanoparticles with multilayer graphene oxide as a spacer for surface enhanced Raman spectroscopy analysis. *Nanoscale* **2018**, *10*, 5897−5905.
(12) Pu, H.; Huang, Z.; Xu, F.; Sun, D. W. Two-dimensional self-assembled Au-Ag core-shell nanorods nanoarray for sensitive detection of thiram in apple using surface-enhanced Raman spectroscopy. *Food Chem.* **2021**, *343*, 128548.
(13) Ren, X.; Li, X. Flower-like Ag coated with molecularly imprinted polymers as a surface-enhanced Raman scattering substrate for the sensitive and selective detection of glibenclamide. *Anal. Methods* **2020**, *12*, 2858−2864.
(14) Lin, S.; Hasi, W.; Han, S.; Lin, X.; Wang, L. Facile fabrication of PS/Cu_2S/Ag sandwich structure as SERS substrate for ultra-sensitive detection. *Spectrochim. Acta A Mol. Biomol. Spectrosc* **2022**, *265*, 120370.
(15) Zhou, N.; Meng, G.; Huang, Z.; Ke, Y.; Zhou, Q.; Hu, X. A flexible transparent Ag-NC@PE film as a cut-and-paste SERS substrate for rapid in situ detection of organic pollutants. *Analyst* **2016**, *141*, 5864−5869.
(16) Zhu, T.; Sun, Y.; Lu, W.; Wang, G.; Zhang, X.; Chen, S.; Zhang, C.; Li, Z.; Man, B.; Yang, C. Theoretical and experimental investigation of the flexible Ag nano-tree@Cu mesh SERS substrate. *J. Alloy. Compd* **2022**, *908*, 164622.
(17) Lin, S.; Hasi, W.; Han, S.; Lin, X.; Wang, L. A dual-functional PDMS-assisted paper-based SERS platform for the reliable detection of thiram residue both on fruit surfaces and in juice. *Anal. Methods* **2020**, *12*, 2571−2579.
(18) Lu, S.; You, T.; Yang, N.; Gao, Y.; Yin, P. Flexible SERS substrate based on Ag nanodendrite-coated carbon fiber cloth: simultaneous detection for multiple pesticides in liquid droplet. *Anal. Bioanal. Chem.* **2020**, *412*, 1159−1167.
(19) Gong, X.; Tang, M.; Gong, Z.; Qiu, Z.; Wang, D.; Fan, M. Screening pesticide residues on fruit peels using portable Raman spectrometer combined with adhesive tape sampling. *Food Chem.* **2019**, *295*, 254−258.
(20) Luo, J.; Wang, Z.; Li, Y.; Wang, C.; Sun, J.; Ye, W.; Wang, X.; Shao, B. Durable and flexible Ag-nanowire-embedded PDMS films for the recyclable swabbing detection of malachite green residue in fruits and fingerprints. *Sens. Actuators B-Chem.* **2021**, *347*, 130602.
(21) Ling, X.; Xie, L.; Fang, Y.; Xu, H.; Zhang, H.; Kong, J.; Dresselhaus, M. S.; Zhang, J.; Liu, Z. Can Graphene be used as a substrate for Raman Enhancement? *Nano Lett.* **2010**, *10*, 553−561.
(22) Ouyang, L.; Yao, L.; Zhou, T.; Zhu, L. Accurate SERS detection of malachite green in aquatic products on basis of graphene wrapped flexible sensor. *Anal. Chim. Acta* **2018**, *1027*, 83−91.
(23) Lai, H.; Xu, F.; Zhang, Y.; Wang, L. Recent progress on graphene-based substrates for surface-enhanced Raman scattering applications. *J. Mater. Chem. B* **2018**, *6*, 4008−4028.
(24) Hu, Y.; López-Lorente, N. I.; Mizaikoff, B. Graphene-based surface enhanced vibrational spectroscopy: recent developments, challenges, and applications. *ACS Photonics* **2019**, *6*, 2182−2193.
(25) Liang, X.; Liang, B.; Pan, Z.; Lang; Zhang, X. Y.; Wang, G.; Yin, P.; Guo, L. Tuning plasmonic and chemical enhancement for SERS detection on graphene-based Au hybrids. *Nanoscale* **2015**, *7*, 20188−20196.
(26) Han, Y.; Han, Y.; Sun, J.; Liu, H.; Luo, X.; Zhang, Y.; Han, L. Controllable Nanoparticle Aggregation through a Superhydrophobic Laser-Induced Graphene Dynamic System for Surface-Enhanced Raman Scattering Detection. *ACS Appl. Mater. Interfaces* **2022**, *14*, 3504−3514.
(27) Nair, A. K.; Sukumaran, K. M.; Thomas, S.; Rouxel, D. D.; Alwarappan, S.; Kalarikkal, N. In Situ Synthesis of Silver Nanospheres, Nanocubes, and Nanowires over Boron-Doped Graphene Sheets for Surface-Enhanced Raman Scattering Application and Enzyme-Free Detection of Hydrogen Peroxide. *Langmuir* **2018**, *34*, 13603−13614.
(28) Dimiev, A. M.; Ceriotti, G.; Behabtu, N.; Zakhidov, D.; Pasquali, M.; Saito, R.; Tour, J. M. Direct real-time monitoring of stage transitions in graphite intercalation compounds. *ACS Nano* **2013**, *7*, 2773−2780.
(29) Cao, L.; Zhu, S.; Pan, B.; Dai, X.; Zhao, W.; Liu, Y.; Xie, W.; Kuang, Y.; Liu, X. Stable and durable laser-induced graphene patterns embedded in polymer substrates. *Carbon* **2020**, *163*, 85−94.
(30) Parthibavarman, M.; Bhuvaneshwari, S.; Jayashree, M.; BoopathiRaja, R. Green synthesis of silver (Ag) nanoparticles using extract of apple and grape and with enhanced visible Light photocatalytic activity. *Bionanoscience* **2019**, *9*, 423−432.
(31) Liu, C.; Xu, X.; Wang, C.; Qiu, G.; Ye, W.; Li, Y.; Wang, D. ZnO/Ag nanorods as a prominent SERS substrate contributed by synergistic charge transfer effect for simultaneous detection of oral antidiabetic drugs pioglitazone and phenformin. *Sens. Actuators B-Chem.* **2020**, *307*, 127634.
(32) Liu, Z.; Li, S.; Hu, C.; Zhang, W.; Zhong, H.; Guo, Z. pH-dependent surface-enhanced Raman scattering of aromatic molecules on graphene oxide. *J. Raman Spectrosc.* **2013**, *44*, 75−80.
(33) Kim, J.; Cote, L. J.; Kim, F.; Huang, J. Visualizing graphene based sheets by fluorescence quenching microscopy. *J. Am. Chem. Soc.* **2010**, *132*, 260−267.
(34) Chen, S.; Ding, C.; Lin, Y.; Wu, Z.; Yuan, W.; Meng, X.; Su, W.; Zhang, K. SERS-active substrate assembled by Ag NWs embedded porous polystyrene fibers. *JRSC Adv.* **2020**, *10*, 21845.
(35) Ma, Y.; Du, Y.; Chen, Y.; Gu, C.; Jiang, T.; Wei, G.; Zhou, J. Intrinsic Raman signal of polymer matrix induced quantitative multiphase SERS analysis based on stretched PDMS film with anchored Ag nanoparticles/Au nanowires. *J. Chem. Eng. J.* **2020**, *381*, 122710.
(36) Xu, H.; Zhu, J.; Wu, X.; Cheng, Y.; Wang, D.; Cai, D. Recognition and quantitative analysis for six phthalate esters (PAEs) through functionalized ZIF-67@Ag nanowires as surface-enhanced Raman scattering substrate. *J. Spectrochim Acta A* **2023**, *284*, 121735.
(37) Tang, L.; Wu, J.; Liu, X.; Su, Q.; Yin, X.; Huang, Z.; Lin, X.; Lin, W.; Yi, G. Au-Nanoparticle-Array/Aligned-Ag-Nanowire-Based Flexible Dual Plasmonic Substrate for Sensitive Surface-Enhanced Raman Scattering Detection. *J. Part Part Syst. Char* **2021**, *38*, 2100160.
(38) Wang, S. Q.; Sun, B.; Jiang, H. Y.; Jin, y.; Feng, J. J.; An, F.; Wang, H. Z.; Xu, W. Facile and robust fabrication of hierarchical Au nanorods /Ag nanowire SERS substrates for the sensitive detection of dyes and pesticides. *Anal. Methods* **2022**, *14*, 1041−1050.
(39) Li, J.; Zhang, W.; Lei, H.; Li, B. Ag nanowire/nanoparticle-decorated MoS2 monolayers for surface-enhanced Raman scattering applications. *J. Nano Res.* **2018**, *11*, 2181−2189.
(40) Pandey, P.; Vongphachanh, S.; Yoon, J.; Kim, B.; Choi, C.-J.; Sohn, J. I.; Hong, W.-K. Silver nanowire-network-film-coated soft substrates with wrinkled surfaces for use as stretchable surface enhanced Raman scattering sensors. *J. Alloys Compd.* **2021**, *859*, 157862.
(41) Li, Z.; Huang, X.; Lu, G. Recent developments of flexible and transparent SERS substrates. *J. Mater. Chem. C* **2020**, *8*, 3956−3969.
(42) Li, X.; Liu, H.; Gu, C.; Zhang, J.; Jiang, T. PDMS/TiO_2/Ag hybrid substrate with intrinsic signal and clean surface for recyclable and quantitative SERS sensing. *Sens. Actuators B: Chem.* **2022**, *351*, 130886.
(43) Mao, Y.; Zhao, Q.; Pan, T.; Shi, J.; Jiang, S.; Chen, M.; Zhou, B.; Tian, Y. Platinum porphyrin/3-(trimethoxysily) propylmethacrylate functionalized flexible PDMS micropillar arrays as optical oxygen sensors. *New J. Chem.* **2017**, *41*, 5429−5435.
(44) Weng, J.; Zhao, S.; Li, Z.; Ricardo, K. B.; Zhou, F.; Kim, H.; Liu, H. Raman enhancement and photo-bleaching of organic dyes in the presence of chemical vapor deposition-grown graphene. *Nanomaterials* **2017**, *7*, 337.
(45) Xu, W.; Mao, N.; Zhang, J. Graphene: a platform for surface-enhanced Raman spectroscopy. *Small* **2013**, *9*, 1206−1224.

https://doi.org/10.1021/acsapm.2c02011
ACS Appl. Polym. Mater. 2023, 5, 2336−2344

(46) Goncalves, L. M.; Valente, I. M.; Rodrigues, J. A. Recent advances in membrane-aided extraction and separation for analytical purposes. *Sep. Purif. Rev.* **2017**, *46*, 179−194.
(47) Ekezie, F. G. C.; Sun, D. W.; Cheng, J. H. Acceleration of microwave-assisted extraction processes of food components by integrating technologies and applying emerging solvents: A review of latest developments. *Trends Food Sci. Technol.* **2017**, *67*, 160−172.
(48) Sun, H.; Ge, X.; Lv, Y.; Wang, A. Application of accelerated solvent extraction in the analysis of organic contaminants, bioactive and nutritional compounds in food and feed. *J. Chromatogr. A* **2012**, *1237*, 1−23.
(49) Tabani, H.; Nojavan, S.; Alexovič, M.; Sabo, J. Recent developments in green membrane-based extraction techniques for pharmaceutical and biomedical analysis. *J. Pharm. Biomed. Anal* **2018**, *160*, 244−267.
(50) Lin, J.; Zhang, C.; Xu, M.; Yuan, Y.; Yao, J. Surface-enhanced Raman spectroscopic identification in fingerprints based on adhesive Au nanofilm. *RSC Adv.* **2018**, *8*, 24477−24484.

Recommended by ACS

Stretchable and Flexible Micro–Nano Substrates for SERS Detection of Organic Dyes
Yuanhang Tan, Changguo Xue, *et al.*
APRIL 11, 2023
ACS OMEGA
READ

Ag/ZIF-8 Substrate with Enhanced SERS via the Plasmonic Nanogap and MOF-Enabled Molecular Preconcentration Effect
Di Cheng, Jin Wang, *et al.*
FEBRUARY 09, 2023
THE JOURNAL OF PHYSICAL CHEMISTRY C
READ

Aerosol Jet Printed Surface-Enhanced Raman Substrates: Application for High-Sensitivity Detection of Perfluoroalkyl Substances
Colleen McDonnell, Rahul Rao, *et al.*
DECEMBER 20, 2022
ACS OMEGA
READ

Flexible SERS Substrate with a Ag–SiO_2 Cosputtered Film for the Rapid and Convenient Detection of Thiram
Longjie Liang, Yongjun Zhang, *et al.*
NOVEMBER 04, 2022
LANGMUIR
READ

Get More Suggestions >

https://doi.org/10.1021/acsapm.2c02011
ACS Appl. Polym. Mater. 2023, 5, 2336−2344